

DETC2003/VIB-48342

FORMULATION OF MULTIBODY DYNAMICS AS COMPLEMENTARITY PROBLEMS

J.C. Trinkle

Department of Computer Science
Rensselaer Polytechnic Institute
110 8th Street
Troy, NY 12180-3590
Email: trinkle@cs.rpi.edu

ABSTRACT

Multibody systems with rigid bodies and unilateral contacts are difficult to simulate due to discontinuities associated with gaining and losing contacts and stick-slip transitions. Methods for simulating such systems fall into two categories: penalty methods and complementarity methods. The former calculate penetration depths of virtual rigid bodies at every time step and compute restoring forces to repair penetrations, while the latter assume that the bodies are truly rigid and compute contact forces that prevent penetration from occurring at all.

In this paper, we are concerned with complementarity methods. We present an instantaneous formulation of the equations of motion of multi-rigid-body systems with frictional contacts as a complementarity problem. The unknowns in this formulation are accelerations and forces at the contacts. Since it is known that this model does not always admit a finite solution, it is problematic to use it directly in an integration scheme. This fact motivates the discrete-time formulation presented second. Although the discrete-time formulation also takes the form of a complementarity problem, it does not suffer from non-existence, and thus it is suitable for simulation. Numerical results are compared to the exact solution for a sphere initially sliding, then rolling, on a horizontal plane.

1 Introduction

Multibody dynamic systems for which the interacting bodies are nominally rigid are ubiquitous in our society: motors, en-

gines, and the automation devices used to build portions of these machines are common examples. Where possible, machine designers use joints that provide bilateral kinematic constraints between the connected bodies (*e.g.*, revolute joints). Such joints are desired, because they are easy to analyze, and they have long operational lives. In some situations, however, design constraints dictate the use of “joints” which provide only unilateral kinematic constraints. For example, in the domain of automated manufacturing, parts feeders typically have rigid protrusions that interact with parts as they stream by (see Figure 1). In assembly applications, fixtures are designed to hold parts in precise positions and orientations relative to each other. If a part comes to rest before fully engaging the fixture, subsequent operations on the fixtured parts may not meet design specifications and may not be recognized until the completed product fails an inspection test.

Despite the importance of multi-rigid-body dynamic systems with unilateral contacts, robust, efficient simulation methods are not widely available. The two primary methods are penalty methods and complementarity methods. The former calculate penetration depths of virtual rigid bodies at every time step and compute restoring forces as functions of these depths to prevent unrealistic penetrations, while the latter assume that the bodies are truly rigid and attempt to compute contact forces that prevent penetration from occurring at all.

The objective of this paper is to present two complementarity formulations of multibody dynamic systems that have served both to increase our theoretical understanding [8] of multibody

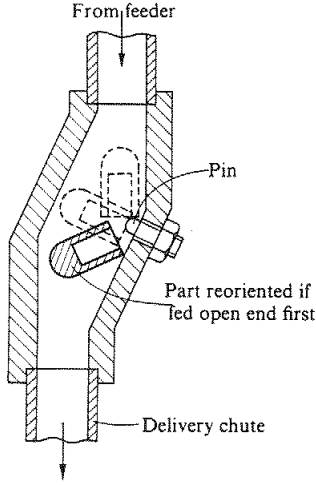


Figure 1. The exit orientation of the cup-shaped part must be with the curved portion down, regardless of the entering orientation [2].

dynamics problems and to provide us with mathematically well-posed and well-behaved time-stepping methods as alternatives to penalty methods.

2 The Model

Our model consists of five parts: the Newton-Euler equation [5], a kinematic map (to relate orientation parameters to angular velocity variables), equality constraints (to model joint connections), a normal contact condition (to model intermittent contact behavior), and a dry friction law satisfying the Maximum Work Principle [4]. To formulate the instantaneous equations of motion, we first introduce the unknowns and several other useful quantities. Let the position and orientation of body j in an inertial frame be represented by the vector \mathbf{q}_j ¹. Three elements of \mathbf{q}_j represent the position of the center of mass of body j and three or more other coordinates² represent the orientation of body j . The generalized velocity of the body's center of mass will be denoted by $\mathbf{v}_j \in \mathbb{R}^6$. The generalized coordinates and velocity of the system, $(\mathbf{q}$ and \mathbf{v}), are constructed by concatenating all the individual body configuration and velocity vectors \mathbf{q}_j and \mathbf{v}_j . Time will be denoted by t .

We assume that two types of contacts exist: permanent mechanical joints, each represented by a system of equality constraints (five in the case of a one-degree-of-freedom joint such as the one shown in Figure 2), and isolated point contacts with well-defined contact normals, each represented by a single inequality constraint (see Figure 2). The former and latter types

¹The tuple \mathbf{q}_j is really not an element of a vector space, but we will refer to it and the related tuple \mathbf{q} as vectors for brevity

²For example, one might choose to use four Euler parameters to represent the orientation of each body.

are also known as bilateral and unilateral contacts, respectively. Let \mathcal{B} and \mathcal{U} denote the mutually exclusive sets of unilateral and bilateral contacts:

$$\mathcal{B} = \{i : \text{contact } i \text{ is a joint}\} \quad (1)$$

$$\mathcal{U} = \{i : \text{contact } i \text{ is a point contact}\}, \quad (2)$$

where $\mathcal{B} \cup \mathcal{U} = \{1, \dots, n_c\}$ and n_c is the number of contacts.

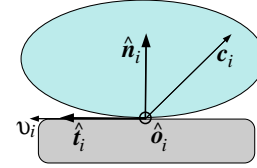


Figure 2. Two bodies in unilateral contact at a point with a well-defined unit normal $\hat{\mathbf{n}}_i$. The orthogonal unit vectors $\hat{\mathbf{t}}_i$ and $\hat{\mathbf{o}}_i$ lie in the contact tangent plane.

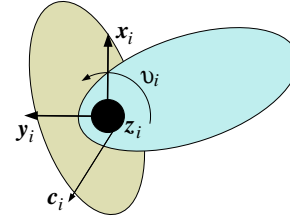


Figure 3. Two bodies joined by a revolute joint. The z_i -axis is co-linear with the joint axis.

In order to define contact maintenance, sliding, and rolling, let $\mathbf{v}_i, \mathbf{c}_i \in \mathbb{R}^6$ denote the relative generalized velocity and force at contact i . These quantities are shown in Figures 2 and 2 for a unilateral and a bilateral contact. The relative velocity at the unilateral contact between the bodies on the left lies in the contact tangent plane (spanned by the orthogonal unit vectors $\hat{\mathbf{t}}_i$ and $\hat{\mathbf{o}}_i$ ($\hat{\mathbf{o}}_i$ points out of the page)), so the bodies are sliding. Since friction is present, the contact force \mathbf{c}_i has both normal and tangential components. The contact frame of the joint is centered on the axis of rotation with the z -axis co-linear with the axis of rotation. Note that the generalized contact force is shown not passing through the center of the joint, thus indicating the presence of friction.

It is convenient to define “normal” and “frictional” subspaces of the generalized relative velocity and the force at a contact. Let \mathbf{v}_{in} and \mathbf{v}_{if} represent orthogonal subspaces of the space

of relative velocities of the bodies at the contact. Specifically, \mathbf{v}_{in} represents the relative velocities normal to the constraints (*i.e.*, those that will be resisted by the structures of the bodies), and \mathbf{v}_{if} represents the relative velocities that are unconstrained but resisted by friction. In terms of these quantities, a contact is said to be maintained if the bodies are touching and if $\mathbf{v}_{in} = 0$ (this will always be true for joints). The mutually exclusive sets of sliding and rolling contacts are defined at the velocity level as:

$$\mathcal{S} = \{i : \mathbf{v}_{in} = 0, \mathbf{v}_{if} \neq 0\} \quad (3)$$

$$\mathcal{R} = \{i : \mathbf{v}_{in} = 0, \mathbf{v}_{if} = 0\}. \quad (4)$$

Note that these definitions apply to unilateral and bilateral contacts.

In analogy to the definitions of \mathbf{v}_{in} and \mathbf{v}_{if} , let \mathbf{c}_{in} represent the components of the generalized contact force that maintain the (unilateral or bilateral) constraints at contact i and let \mathbf{c}_{if} represent the generalized friction force at contact i .

We are now in a position to develop the system of equations defining the dynamic motion of multi-rigid-body systems. Recall the five parts mentioned above.

1. **Newton-Euler Equations:** The Newton-Euler equation can be written as follows:

$$\mathbf{M}(\mathbf{q})\dot{\boldsymbol{\nu}} = \mathbf{g}(\mathbf{q}, \boldsymbol{\nu}, t), \quad (5)$$

where $\mathbf{M}(\mathbf{q})$ is the inertia tensor and $\mathbf{g}(\mathbf{q}, \boldsymbol{\nu}, t)$ is the vector of loads experienced by the bodies.

2. **Kinematic Map:** The time rate of change of the generalized coordinates $\dot{\mathbf{q}}$ must be related to the generalized velocity of the bodies $\boldsymbol{\nu}$:

$$\dot{\mathbf{q}} = \mathbf{G}(\mathbf{q})\boldsymbol{\nu}. \quad (6)$$

Note that when the orientation representation uses more than three parameters, \mathbf{G} is not square, although it has the property that $\mathbf{G}^T \mathbf{G} = \mathbf{I}$, where \mathbf{I} is the identity matrix of the appropriate size.

3. **Joint Constraints:** If contact i is a joint (*i.e.*, $i \in \mathcal{B}$), there is a vector constraint function denoted by ${}^b\psi_{in}(\mathbf{q}, t) = 0$. Stacking the ${}^b\psi_{in}$ functions for all $i \in \mathcal{B}$ into the vector ${}^b\boldsymbol{\Psi}_n(\mathbf{q}, t)$, the system constraints can be written as follows:

$${}^b\boldsymbol{\Psi}_n(\mathbf{q}, t) = 0. \quad (7)$$

4. **Normal Contact Constraints:** For each unilateral contact, one can define a signed distance or gap function, ${}^u\psi_{in}(\mathbf{q}, t)$

for all $i \in \mathcal{U}$, which is zero as long as the bodies in question remain in contact and becomes greater than zero when they separate. Since the bodies are rigid, they may never overlap. Thus the gap functions are constrained to be nonnegative. Stacking all the gap functions into the vector ${}^u\boldsymbol{\Psi}_n(\mathbf{q}, t)$ yields the following nonpenetration constraint:

$${}^u\boldsymbol{\Psi}_n(\mathbf{q}, t) \geq 0. \quad (8)$$

This constraint applies only locally in the configuration space of the system.

The force at each contact is assumed to be compressive. That is, the normal component of the force at contact i may not act to pull the bodies together (*i.e.*, ${}^u\mathbf{c}_{in} \geq 0$). Combining all ${}^u\mathbf{c}_{in}$ for all $i \in \mathcal{U}$ into the vector ${}^u\mathbf{c}_n$, we write all normal force constraints as:

$${}^u\mathbf{c}_n \geq 0. \quad (9)$$

Note that ${}^u\mathbf{c}_{in}$ acts to prevent ${}^u\psi_{in}$ from becoming negative and thus may be regarded as a Lagrange multiplier.

There is one last constraint needed to properly represent the disjunctive nature of unilateral contact interactions. More specifically, if the contact is supporting a load (*i.e.*, ${}^u\mathbf{c}_{in} > 0$), then the contact must be maintained (*i.e.*, ${}^u\psi_{in} = 0$). Conversely, if the contact breaks (*i.e.*, ${}^u\psi_{in} > 0$), then the normal components (and hence the frictional components too) of the contact force must be zero (*i.e.*, ${}^u\mathbf{c}_{in} = 0$). At least one of ${}^u\mathbf{c}_{in}$ and ${}^u\psi_{in}$ must be zero. Notice these conditions imply the orthogonality of the vectors ${}^u\mathbf{c}_n$ and ${}^u\boldsymbol{\Psi}_n(\mathbf{q}, t)$:

$${}^u\boldsymbol{\Psi}_n(\mathbf{q}, t)^T {}^u\mathbf{c}_n = 0 \quad (10)$$

where the superscript T is the transpose operator.

5. **Friction Law:** At contact i , the generalized friction force \mathbf{c}_{if} can act only in a subset of the unconstrained directions and must lie within a closed convex limit set $\mathcal{F}_i(\mathbf{c}_{in}, \mu_i)$. The limit set must contain the origin³ and typically scales with the normal component of the contact force and friction coefficient μ_i , thus forming a friction cone. When contact i is rolling, the friction force may take on any value within the set. However, when the contact is sliding, the friction force must be the one within $\mathcal{F}_i(\mathbf{c}_{in}, \mu_i)$ that maximizes the energy dissipation. Such models are said to satisfy the Maximum Work Principle [4], which can be expressed as follows:

$$\mathbf{c}_{if} \in \operatorname{argmax} \{ -\mathbf{v}_{if}^T \mathbf{c}'_{if} : \mathbf{c}'_{if} \in \mathcal{F}_i(\mathbf{c}_{in}, \mu_i) \}, \quad (11)$$

³If the origin is not in \mathcal{F}_i , then the maximally dissipative friction force at a sliding contact can generate energy in some sliding directions. Convexity of \mathcal{F}_i guarantees that the friction force direction at a sliding contact is unique.

where \mathbf{c}'_{if} is an arbitrary vector in the set $\mathcal{F}_i(\mathbf{c}_{in}, \mu_i)$. For example, if contact i is a unilateral point contact with isotropic Coulomb friction, then the scalar ${}^u c_{in}$ denotes the normal component of the contact force and ${}^u v_{in}$ is zero. The friction force is denoted by ${}^u \mathbf{c}_{if} = ({}^u c_{it}, {}^u c_{io})$ and the tangential relative velocity ${}^u \mathbf{v}_{if} = ({}^u v_{it}, {}^u v_{io})$ lie in the contact tangent plane. The friction limit set $\mathcal{F}_i({}^u c_{in}, \mu_i)$ is the disc defined as follows (see Figure 4):

$$\mathcal{F}_i({}^u c_{in}, \mu_i) = \{ {}^u \mathbf{c}_{if} : \| {}^u \mathbf{c}_{if} \| \leq \mu_i {}^u c_{in}, {}^u c_{in} \geq 0 \}, \quad (12)$$

where $\|(\cdot)\|$ denotes the Euclidean norm and μ_i is the non-negative coefficient of friction. Maximum work occurs when the friction force is opposite to the relative velocity, as shown in Figure 4.

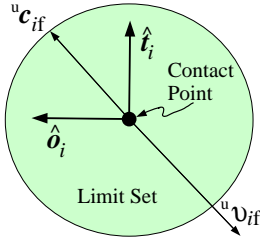


Figure 4. Circular limit set of radius $\mu_i {}^u c_{in}$ in the contact tangent plane for isotropic Coulomb friction. The contact point is at the center of the circle. A nonzero relative velocity component in the contact tangent plane ${}^u \mathbf{v}_{if}$ gives rise to the maximally dissipative friction force ${}^u \mathbf{c}_{if}$.

Our instantaneous dynamic model is defined by equations (5,6,7,8,9,10,11), but the equations are in a form that makes their solution difficult. However, as will be shown, the model can be cast as a complementarity problem [3], allowing one to apply well-studied, solution algorithms.

Complementarity Problems The standard nonlinear complementarity problem (NCP) can be stated as follows:

Definition 1. Nonlinear Complementarity Problem (NCP): Given an unknown vector $\mathbf{z} \in \mathbb{R}^m$ and a known vector function $\mathbf{w}(\mathbf{z}) : \mathbb{R}^m \rightarrow \mathbb{R}^m$, determine \mathbf{z} such that:

$$0 \leq \mathbf{w}(\mathbf{z}) \perp \mathbf{z} \geq 0, \quad (13)$$

where \perp implies orthogonality (i.e., $\mathbf{w}(\mathbf{z})^T \mathbf{z} = 0$).

The standard linear complementarity problem is a special case:

Definition 2. Linear Complementarity Problem (LCP): Given an unknown vector $\mathbf{z} \in \mathbb{R}^m$, a known fixed matrix $\mathbf{F} \in \mathbb{R}^{m \times m}$, and a known fixed vector $\mathbf{f} \in \mathbb{R}^m$, determine \mathbf{z} such that:

$$\mathbf{w} = \mathbf{F}\mathbf{z} + \mathbf{f} \quad (14)$$

$$0 \leq \mathbf{w} \perp \mathbf{z} \geq 0. \quad (15)$$

We adopt the shorthand notation, $\text{LCP}(\mathbf{F}, \mathbf{f})$.

2.1 Complementarity Formulation of the Instantaneous Model

To achieve model formulation as a well-posed complementarity problem, we must take three steps. First, express the Maximum Work Principle as a system of equations and inequalities, second, express all relevant equations in terms of accelerations, and third, expose the contact forces in the Newton-Euler equation. The unknowns of the resulting complementarity problem will be accelerations and contact forces.

1. **Reformulating the Maximum Work Principle:** The Maximum Work Principle (11) can be replaced by an equivalent system of equations and inequalities by formulating it as an unconstrained optimization problem with Lagrange multipliers and applying Fritz-John optimality conditions. However, to do this, a specific form of \mathcal{F}_i is required. In this paper, we will consider only two simplified friction models; isotropic Coulomb friction at unilateral contacts and dry friction of constant maximum magnitude in one-degree-of-freedom joints.

At unilateral contacts, we will assume isotropic Coulomb friction as defined in the example above. If contact i is a one-degree-of-freedom joint, we will assume that the maximum magnitude of the dry friction force is independent of the load in the other five component directions. Thus the friction limit set for a bilateral joint $\mathcal{F}_i(\mu_i)$ will be:

$$\mathcal{F}_i({}^b c_{if \max}) = \{ {}^b c_{if} : |{}^b c_{if}| \leq {}^b c_{if \max} \}, \quad \forall i \in \mathcal{B}, \quad (16)$$

where $|(\cdot)|$ denotes the absolute value of a scalar and ${}^b c_{if \max}$ is the nonnegative maximum magnitude of the generalized friction force in joint i . Such a limit set can be seen as a special case of the circular limit set for unilateral contact. If one fixes the diameter of the circle and removes the t -direction, the limit set reduces to a line segment (in the direction of joint travel) of fixed length ${}^b c_{if \max}$.

Applying the Fritz-John optimality conditions to equation (11) with \mathcal{F}_i given by equation (12) yields the following equivalent system:

$$\left. \begin{aligned} \mu_i {}^u c_{in} {}^u v_{it} + {}^u c_{it} {}^u \lambda_i &= 0 \\ \mu_i {}^u c_{in} {}^u v_{io} + {}^u c_{io} {}^u \lambda_i &= 0 \\ {}^u s_i = \mu_i^2 {}^u c_{in}^2 - {}^u c_{it}^2 - {}^u c_{io}^2 &\geq 0 \\ 0 \leq {}^u s_i \perp {}^u \lambda_i &\geq 0 \end{aligned} \right\} \forall i \in \mathcal{U} \quad (17)$$

where ${}^u \lambda_i$ is the Lagrange multiplier of the constraint and ${}^u s_i$ is a slack variable for the friction limit set. Note that ${}^u \lambda_i = \|{}^u \mathbf{v}_{if}\|$ at an optimal solution.

The result obtained when \mathcal{F}_i is given by equation (16) is:

$$\left. \begin{aligned} {}^b c_{if\max} {}^b v_{if} + {}^b c_{if} {}^b \lambda_i &= 0 \\ {}^b s_i = {}^b c_{if\max}^2 - {}^b c_{if}^2 &\geq 0 \\ 0 \leq {}^b s_i \perp {}^b \lambda_i &\geq 0 \end{aligned} \right\} \forall i \in \mathcal{B} \quad (18)$$

Note that ${}^b \lambda_i = |{}^b v_{if}|$ at an optimal solution.

2. Writing Contact Constraints in Terms of Accelerations:

Equation (7) is expressed at the acceleration level by differentiating twice with respect to time:

$${}^b \mathbf{a}_n = {}^b \mathbf{W}_n^T \dot{\boldsymbol{\nu}} + {}^b \mathbf{k}(\mathbf{q}, \boldsymbol{\nu}, t) = 0, \quad (19)$$

where ${}^b \mathbf{W}_n^T = \frac{\partial ({}^b \boldsymbol{\Psi}_n)}{\partial \mathbf{q}} \mathbf{G}$ and

$${}^b \mathbf{k}(\mathbf{q}, \boldsymbol{\nu}, t) = {}^b \dot{\mathbf{W}}_n^T \boldsymbol{\nu} + \frac{\partial^2 ({}^b \boldsymbol{\Psi}_n)}{\partial \mathbf{q} \partial t} \mathbf{G} \boldsymbol{\nu} + \frac{\partial^2 ({}^b \boldsymbol{\Psi}_n)}{\partial t^2}.$$

Equation (8) can be expressed in terms of accelerations in the same way:

$${}^u \mathbf{a}_n = {}^u \mathbf{W}_n^T \dot{\boldsymbol{\nu}} + {}^u \mathbf{k}(\mathbf{q}, \boldsymbol{\nu}, t) \geq 0 \quad (20)$$

where ${}^u \mathbf{W}_n^T = \frac{\partial ({}^u \boldsymbol{\Psi}_n)}{\partial \mathbf{q}} \mathbf{G}$ and

$${}^u \mathbf{k}(\mathbf{q}, \boldsymbol{\nu}, t) = {}^u \dot{\mathbf{W}}_n^T \boldsymbol{\nu} + \frac{\partial^2 ({}^u \boldsymbol{\Psi}_n)}{\partial \mathbf{q} \partial t} \mathbf{G} \boldsymbol{\nu} + \frac{\partial^2 ({}^u \boldsymbol{\Psi}_n)}{\partial t^2}.$$

However, note that this constraint only applies for each unilateral contact whose normal component of velocity zero (*i.e.*, $i \in \mathcal{U} \cup (\mathcal{S} \cup \mathcal{R})$).

We can now express equations (8-10) in terms of accelerations:

$$0 \leq {}^u \mathbf{c}_n \perp {}^u \mathbf{a}_n \geq 0. \quad (21)$$

The Maximum Work Principle (11) must be considered further. When contact i is sliding, the solutions of conditions (17) and (18) produce the correct results (*i.e.*, the friction force obtains its maximum magnitude and directly opposes the sliding direction) and, we can use these conditions to eliminate ${}^u c_{if}$. Also as required, when a contact is

rolling, these conditions allow the friction force to lie anywhere within the friction limit set. What these conditions do not provide is a mechanism for determining if a rolling contact will transition to sliding. However, this problem is easily remedied by replacing the relative velocity variables in equation (11) with the analogous acceleration variables.

$$\left. \begin{aligned} \mu_i {}^u c_{in} {}^u a_{it} + {}^u c_{it} {}^u \lambda_i &= 0 \\ \mu_i {}^u c_{in} {}^u a_{io} + {}^u c_{io} {}^u \lambda_i &= 0 \\ {}^u s_i = \mu_i^2 {}^u c_{in}^2 - {}^u c_{it}^2 - {}^u c_{io}^2 &\geq 0 \\ 0 \leq {}^u s_i \perp {}^u \lambda_i &\geq 0 \end{aligned} \right\} \forall i \in \mathcal{U} \cap \mathcal{R} \quad (22)$$

where ${}^u \lambda_i = \|{}^u \mathbf{a}_{if}\|$ at and optimal solution.

$$\left. \begin{aligned} {}^b c_{if\max} + {}^b c_{if} {}^b \lambda_i &= 0 \\ {}^b s_i = {}^b c_{if\max}^2 - {}^b c_{if}^2 &\geq 0 \\ 0 \leq {}^b s_i \perp {}^b \lambda_i &\geq 0 \end{aligned} \right\} \forall i \in \mathcal{B} \cap \mathcal{R} \quad (23)$$

where ${}^b \lambda_i = |{}^b a_{if}|$ at and optimal solution.

3. Exposing the Contact Forces in the Newton-Euler Equation:

Recall that the vector $\mathbf{g}(\mathbf{q}, \boldsymbol{\nu}, t)$ represents the resultant generalized forces acting on the bodies. In order to complete the formulation as an NCP, $\mathbf{g}(\mathbf{q}, \boldsymbol{\nu}, t)$ is expressed as the sum of the normal and friction forces at the unilateral and bilateral contacts and all other generalized forces. The Newton-Euler equation becomes:

$$\begin{aligned} \mathbf{M}(\mathbf{q}) \dot{\boldsymbol{\nu}} &= {}^u \mathbf{W}_n(\mathbf{q}) {}^u \mathbf{c}_n + {}^u \mathbf{W}_f(\mathbf{q}) {}^u \mathbf{c}_f \\ &+ {}^b \mathbf{W}_n(\mathbf{q}) {}^b \mathbf{c}_n + {}^b \mathbf{W}_f(\mathbf{q}) {}^b \mathbf{c}_f + \mathbf{g}_{\text{ext}}(\mathbf{q}, \boldsymbol{\nu}, t), \end{aligned} \quad (24)$$

where \mathbf{g}_{ext} is the resultant of all non-contact wrenches applied to the bodies, ${}^u \mathbf{c}_f$ and ${}^b \mathbf{c}_f$ are formed by stacking the generalized friction vectors at the unilateral and bilateral contacts respectively, and the matrices ${}^u \mathbf{W}_n$, ${}^u \mathbf{W}_f$, ${}^b \mathbf{W}_n$, and ${}^b \mathbf{W}_f$ map contact forces into a common inertial frame.

2.2 A Differential NCP

The instantaneous dynamic model is now complete.

Definition 3. CP1: Equations (6,17,18,19,21,22,23,24) constitute a differential, nonlinear complementarity problem.

It is known that solutions to CP1 do not always exist (see [8]), however, if the Maximum Work Principle is relaxed so that friction forces merely need to be dissipative, rather than maximally dissipative, then a solution always exists [6]. If one wanted to use this NCP in an integration scheme to simulation the motion

of a multibody system, the *path* algorithm by Ferris and Munson is the most robust, general purpose NCP solver available (www.cs.wisc.edu/cpnet/). One should also note that this NCP can be converted into an approximate LCP by linearizing the friction cone constraint (see [8] for details). The LCP then can be solved by Lemke's algorithm [3], but the solution non-existence problem persists.

In the next section, we will present an Euler time-stepping method formulated as an LCP with guaranteed solution existence.

3 Discrete-Time Formulation as an LCP

Let h denote a positive step size and t_l the current time, for which we have estimates of the configuration $\mathbf{q}^l = \mathbf{q}(t_l)$ and the generalized velocity $\boldsymbol{\nu}^l = \boldsymbol{\nu}(t_l)$ of the system. Our goal is to derive approximations of the configuration $\mathbf{q}^{(l+1)} = \mathbf{q}(t_l + h)$ and velocity $\boldsymbol{\nu}^{(l+1)} = \boldsymbol{\nu}(t_l + h)$ that approximately satisfy the NCP derived in Section 2. In the derivation of the time-stepping subproblem, we assume that the matrices \mathbf{M} , ${}^u\mathbf{W}_n$, ${}^b\mathbf{W}_n$, ${}^u\mathbf{W}_f$, ${}^b\mathbf{W}_f$ and the vector \mathbf{g}_{ext} are constant over the current time step⁴. In addition, we use the following approximations of the state derivatives: $\dot{\boldsymbol{\nu}} \approx (\boldsymbol{\nu}^{(l+1)} - \boldsymbol{\nu}^{(l)})/h$ and $\dot{\mathbf{q}} \approx (\mathbf{q}^{(l+1)} - \mathbf{q}^{(l)})/h$.

1. **Discrete-Time Newton-Euler Equations:** The discrete-time form of the Newton-Euler equation (24) is given as:

$$\begin{aligned} \mathbf{M} \cdot (\boldsymbol{\nu}^{(l+1)} - \boldsymbol{\nu}^{(l)}) &= {}^u\mathbf{W}_n {}^u\mathbf{p}_n^{(l+1)} + {}^u\mathbf{W}_f {}^u\mathbf{p}_f^{(l+1)} \\ &+ {}^b\mathbf{W}_n {}^b\mathbf{p}_n^{(l+1)} + {}^b\mathbf{W}_f {}^b\mathbf{p}_f^{(l+1)} + \mathbf{p}_{\text{ext}}, \end{aligned} \quad (25)$$

where the \cdot on the left side of the equation denotes multiplication and ${}^u\mathbf{p}_n^{(l+1)} = h{}^u\mathbf{c}_n^{(l+1)}$, ${}^u\mathbf{p}_f^{(l+1)} = h{}^u\mathbf{c}_f^{(l+1)}$, ${}^b\mathbf{p}_n^{(l+1)} = h{}^b\mathbf{c}_n^{(l+1)}$, ${}^b\mathbf{p}_f^{(l+1)} = h{}^b\mathbf{c}_f^{(l+1)}$ are the unknown generalized contact impulses. One should notice that since the contact forces are known only at the end of each time interval, the definitions of the impulses imply that we must view the contact forces as constant over each time interval.

2. **Discrete-Time Kinematic Map:** The discrete-time form of the kinematic map (6) is given as follows:

$$\mathbf{q}^{(l+1)} - \mathbf{q}^{(l)} = h\mathbf{G}\boldsymbol{\nu}^{(l+1)}. \quad (26)$$

Note that using $\boldsymbol{\nu}^{(l+1)}$ rather than $\boldsymbol{\nu}^{(l)}$ is consistent with our desire to have the time-stepping subproblem be consistent with all components of the dynamic model at the end of each time step.

⁴This leads to an explicit time-stepping method with each step requiring the solution of an LCP. If this assumption is not made, then the time-stepping method is implicit and requires solving an NCP.

3. **Discrete-Time Joint Constraints:** Denoting ${}^b\Psi_n(\mathbf{q}^{(l)}, t_l)$ by ${}^b\Psi_n^{(l)}$, the Taylor series expansion of the discrete-time joint constraints (7) truncated after the linear terms is:

$${}^b\Psi_n^{(l+1)} \approx {}^b\Psi_n^{(l)} + \frac{\partial {}^b\Psi_n^{(l)}}{\partial \mathbf{q}} (\mathbf{q}^{(l+1)} - \mathbf{q}^{(l)}) + \frac{\partial {}^b\Psi_n^{(l)}}{\partial t} h. \quad (27)$$

Substituting equation (26), the linearized joint constraint (7) becomes:

$${}^b\Psi_n^{(l)} + {}^b\mathbf{W}_n^T \boldsymbol{\nu}^{(l+1)} h + \frac{\partial {}^b\Psi_n^{(l)}}{\partial t} h = 0. \quad (28)$$

4. **Discrete-Time Normal Contact Constraints:** Denoting ${}^u\Psi_n(\mathbf{q}^{(l)}, t_l)$ by ${}^u\Psi_n^{(l)}$, the Taylor series expansion of the constraints (8) truncated after the linear terms is given by:

$${}^u\Psi_n^{(l+1)} \approx {}^u\Psi_n^{(l)} + \frac{\partial {}^u\Psi_n^{(l)}}{\partial \mathbf{q}} (\mathbf{q}^{(l+1)} - \mathbf{q}^{(l)}) + \frac{\partial {}^u\Psi_n^{(l)}}{\partial t} h. \quad (29)$$

Thus in the discrete-time LCP formulation, the nonlinear unilateral contact constraint (8) will be replaced by the following approximate gap expression:

$${}^u\Psi_n^{(l)} + {}^u\mathbf{W}_n^T \boldsymbol{\nu}^{(l+1)} h + \frac{\partial {}^u\Psi_n^{(l)}}{\partial t} h \geq 0. \quad (30)$$

Given that ${}^u\mathbf{p}_n^{(l+1)} = h{}^u\mathbf{c}_n^{(l+1)}$ and ${}^u\mathbf{c}_n \geq 0$, equation (9) can be replaced by:

$${}^u\mathbf{p}_n^{(l+1)} \geq 0. \quad (31)$$

Last, for each unilateral contact, the gap at the end of the time step must be orthogonal to the normal impulse. Combining this fact with constraints (30) and (31) yields the following linear complementarity relationship in ${}^u\mathbf{p}_n^{(l+1)}$ and $\boldsymbol{\nu}^{(l+1)}$:

$$0 \leq {}^u\mathbf{p}_n^{(l+1)} \perp \left({}^u\Psi_n^{(l)} + {}^u\mathbf{W}_n^T \boldsymbol{\nu}^{(l+1)} h + \frac{\partial {}^u\Psi_n^{(l)}}{\partial t} h \right) \geq 0. \quad (32)$$

Note that this relationship implies that the normal impulse ${}^u\mathbf{p}_n^{(l+1)}$ at the end of the time step can be nonzero only if the gap at the end of the time step is zero. Constraint (32) is again consistent with the goal of consistency at the end of each time step.

5. **Discrete-Time Maximum Work Principle:** The friction law will be modified for the discrete-time setting by replacing force variables with impulse variables. Thus equation (11) becomes:

$$\mathbf{p}'_{if}{}^{(l+1)} \in \operatorname{argmax} \left\{ \left(-\mathbf{v}'_{if}{}^{(l+1)} \right)^T \mathbf{p}'_{if} : \mathbf{p}'_{if} \in \mathcal{F}_i(\mathbf{p}'_{in}{}^{(l+1)}, \mu_i) \right\}, \quad (33)$$

where \mathbf{p}'_{if} is an arbitrary vector in the set $\mathcal{F}_i(\mathbf{p}'_{in}{}^{(l+1)}, \mu_i)$. As was the case during the formulation of the instantaneous model, we cannot complete the formulation of the discrete-time model without assuming a particular form of \mathcal{F}_i .

3.1 The Discrete-Time Model as an LCP

Assuming that contact i is unilateral with isotropic Coulomb friction, we have:

$$\mathcal{F}_i(\mathbf{p}'_{in}{}^{(l+1)}, \mu_i) = \{ \mathbf{p}'_{if}{}^{(l+1)} : \|\mathbf{p}'_{if}{}^{(l+1)}\| \leq \mu_i \mathbf{p}'_{in}{}^{(l+1)}, \mathbf{p}'_{in}{}^{(l+1)} \geq 0 \}. \quad (34)$$

Figure 5 shows a circular friction limit set (shown dotted) at a unilateral contact for particular values of $\mathbf{p}'_{in}{}^{(l+1)}$ and μ_i . This circle, of radius $\mu_i \mathbf{p}'_{in}{}^{(l+1)}$, is approximated by a convex polygon containing the origin (e.g., a nonagon as shown in Figure 5). The vertices of the polygon are defined by n_d scaled unit vectors $\mu_i \mathbf{d}_{ij}$ that span the contact tangent plane defined by $\hat{\mathbf{t}}_i$ and $\hat{\mathbf{o}}_i$.

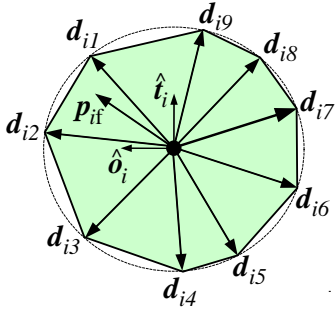


Figure 5. Circular friction limit set approximated by a nonagon.

To constrain the friction impulse $\mathbf{p}'_{if}{}^{(l+1)}$ to lie within the polygonal limit set, it will be represented as the convex sum of vectors \mathbf{d}_{ij} . Letting $\beta_{ij}^{(l+1)}$ denote the barycentric coordinate of $\mathbf{p}'_{if}{}^{(l+1)}$ associated with direction \mathbf{d}_{ij} , the polygon can be represented as follows:

$$\left. \begin{aligned} \mathbf{p}'_{if}{}^{(l+1)} &= \sum_{j=1}^{n_d} \beta_{i,j} \mathbf{d}_{ij} \\ \sum_{j=1}^{n_d} \beta_{i,j} &\leq \mu_i \mathbf{p}'_{in}{}^{(l+1)} \end{aligned} \right\} \quad \forall i \in \mathcal{U}, \quad (35)$$

where ${}^u \mathbf{D}_i$ is the matrix whose j^{th} column is the unit vector \mathbf{d}_{ij} mapped into the configuration space of the system.

It remains to enforce the fact that at a rolling contact, the friction impulse may lie anywhere within the limit set, but while sliding, the friction impulse must maximize power dissipation. This is accomplished through the following constraints:

$$\left. \begin{aligned} 0 &\leq \left({}^u \mathbf{D}_i^T \boldsymbol{\nu}^{(l+1)} + {}^u \mathbf{e}_i {}^u \boldsymbol{\sigma}_i^{(l+1)} \right) \perp {}^u \boldsymbol{\beta}_i^{(l+1)} \geq 0 \\ 0 &\leq \left(\mu_i {}^u \mathbf{p}'_{in}{}^{(l+1)} - {}^u \mathbf{e}_i^T {}^u \boldsymbol{\beta}_i^{(l+1)} \right) \perp {}^u \boldsymbol{\sigma}_i^{(l+1)} \geq 0 \end{aligned} \right\} \quad \forall i \in \mathcal{U} \quad (36)$$

where ${}^u s_i^{(l+1)}$ is a slack variable and ${}^u \mathbf{e}_i$ is a column vector of length n_d with all elements equal to 1. The physical interpretation of the slack variable ${}^u s_i^{(l+1)}$ is an approximation of the magnitude of the sliding velocity at contact i . Given that the conditions (36) are satisfied, when contact i is sliding (i.e., ${}^u s_i^{(l+1)} > 0$), the element of ${}^u \boldsymbol{\beta}_i^{(l+1)}$ corresponding to most direct opposition to the sliding velocity will be nonzero and the magnitude of the tangential impulse will be $\mu_i {}^u p_i^{(l+1)}$. In addition, when contact i is rolling (i.e., ${}^u s_i^{(l+1)} = 0$), multiple elements of ${}^u \boldsymbol{\beta}_i^{(l+1)}$ may be nonzero (typically two elements) and the friction impulse vector may lie anywhere in the polygonal friction limit set.

One important side-affect of the above approximation of the Maximum Work Principle is that an entire cone of relative velocities at contact i lead to exactly the same friction force, because that force maximizes energy dissipation. As the direction of sliding changes, the direction of the friction force jumps from one direction vector to the next (see Figure 6).

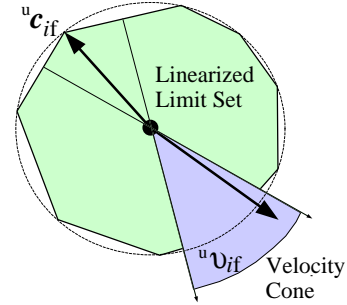


Figure 6. Cone of relative velocities giving rise to the same friction force.

Combining the tangential complementarity conditions for all unilateral contacts yields:

$$\left. \begin{aligned} 0 &\leq \left({}^u \mathbf{D}^T \boldsymbol{\nu}^{(l+1)} + {}^u \mathbf{E} {}^u \boldsymbol{\sigma}^{(l+1)} \right) \perp {}^u \boldsymbol{\beta}^{(l+1)} \geq 0 \\ 0 &\leq \left(\mathbf{U} {}^u \mathbf{p}'_n{}^{(l+1)} - {}^u \mathbf{E}^T {}^u \boldsymbol{\beta}^{(l+1)} \right) \perp {}^u \boldsymbol{\sigma}^{(l+1)} \geq 0 \end{aligned} \right\} \quad (37)$$

where the column vectors ${}^u\boldsymbol{\beta}^{(l+1)}$ and ${}^u\mathbf{s}^{(l+1)}$ are formed by stacking the vectors ${}^u\boldsymbol{\beta}_i^{(l+1)}$ and scalars ${}^u s_i^{(l+1)}$, \mathbf{D}_u^T is formed by stacking the matrices ${}^u\mathbf{D}_i^T$, ${}^u\mathbf{E}$ is a block diagonal matrix with nonzero blocks given by ${}^u\mathbf{e}_i$, and \mathbf{U} is the diagonal matrix with element (i, i) equal to μ_i .

Complementarity constraints for a joint can be written similarly. In the case of a one-degree-of-freedom joint, the space of relative velocities is one-dimensional and thus can be positively spanned by a pair of vectors pointing in opposite directions. We have:

$$\begin{aligned} 0 \leq ({}^b\mathbf{D}^T \boldsymbol{\nu}^{(l+1)} + {}^b\mathbf{E}^b \boldsymbol{\sigma}^{(l+1)}) \perp {}^b\boldsymbol{\beta}^{(l+1)} &\geq 0 \\ 0 \leq ({}^b\boldsymbol{\beta}_{\max} - {}^b\mathbf{E}^T {}^b\boldsymbol{\beta}^{(l+1)}) \perp {}^b\boldsymbol{\sigma}^{(l+1)} &\geq 0 \end{aligned} \quad (38)$$

3.2 A Time-Stepping LCP

A time-stepping LCP is now at hand. Equations (26,28,32,37,38) constitute a mixed LCP⁵. Its solution yields estimates of the contact forces and the generalized velocity of the system at t_{l+1} . This solution can then be substituted into equation (26) to obtain an estimate of the system configuration at t_{l+1} . It is known that solutions always exist to the simplified LCP derived by eliminating joints and by removing the terms ${}^u\Psi_n^{(l)}$ and $\frac{\partial {}^u\Psi_n^{(l)}}{\partial t} h$ from equation (32) (see [1]).

Since \mathbf{M} is symmetric and positive definite, it is invertible, so we can solve equation (26) for $\boldsymbol{\nu}^{(l+1)}$ and eliminate it to yield a smaller mixed LCP. However, under the assumption that the null space of ${}^b\mathbf{W}_n$ is trivial⁶, then the mixed LCP can be converted into a standard LCP. To do this, one solves equations (26) and (28) for $\boldsymbol{\nu}^{(l+1)}$ and ${}^b\mathbf{p}_n^{(l+1)}$ and substitutes the results into equations (32,37,38), which before substitution can be written as follows:

$$0 \leq \begin{bmatrix} {}^u\mathbf{W}_n^T \boldsymbol{\nu}^{(l+1)} + {}^u\Psi_n^{(l)}/h + \frac{\partial {}^u\Psi_n^{(l)}}{\partial t} \\ {}^u\mathbf{D}^T \boldsymbol{\nu}^{(l+1)} + {}^u\mathbf{E} {}^u\mathbf{s}^{(l+1)} \\ {}^b\mathbf{D}^T \boldsymbol{\nu}^{(l+1)} + {}^u\mathbf{E} {}^u\mathbf{s}^{(l+1)} \\ \mathbf{U} {}^u\mathbf{p}_n^{(l+1)} - {}^u\mathbf{E}^T {}^u\boldsymbol{\beta}^{(l+1)} \\ {}^b\boldsymbol{\beta}_{\max} - {}^u\mathbf{E}^T {}^u\boldsymbol{\beta}^{(l+1)} \end{bmatrix} \perp \begin{bmatrix} {}^u\mathbf{p}^{(l+1)} \\ {}^u\boldsymbol{\beta}^{(l+1)} \\ {}^b\boldsymbol{\beta}^{(l+1)} \\ {}^u\mathbf{s}^{(l+1)} \\ {}^b\mathbf{s}^{(l+1)} \end{bmatrix} \geq 0. \quad (39)$$

We first cast equations (26) and (28) into matrix form:

$$\begin{bmatrix} \mathbf{M} & -{}^b\mathbf{W}_n \\ -{}^b\mathbf{W}_n & 0 \end{bmatrix} \begin{bmatrix} \boldsymbol{\nu}^{(l+1)} \\ {}^b\mathbf{p}_n^{(l+1)} \end{bmatrix} = \begin{bmatrix} \mathbf{x}_1 \\ \mathbf{x}_2 \end{bmatrix}, \quad (40)$$

⁵A mixed LCP is an LCP augmented with equations, in our case, equations (26,28)

⁶This is true usually if the bilateral constraints do not generate rigid loops.

where

$$\mathbf{x}_1 = {}^u\mathbf{W}_n {}^u\mathbf{p}_n^{(l+1)} + {}^b\mathbf{D} {}^b\boldsymbol{\beta}^{(l+1)} + {}^u\mathbf{D} {}^u\boldsymbol{\beta}^{(l+1)} + \mathbf{M} \boldsymbol{\nu}^{(l)} + \mathbf{p}_{\text{ext}} \quad (41)$$

$$\mathbf{x}_2 = {}^b\Psi_n^{(l)}/h + \frac{\partial {}^b\Psi_n^{(l)}}{\partial t}. \quad (42)$$

Inverting the matrix on the left side of equation (40) yields:

$$\begin{bmatrix} \boldsymbol{\nu}^{(l+1)} \\ {}^b\mathbf{p}_n^{(l+1)} \end{bmatrix} = \begin{bmatrix} \mathbf{A}_{11} & \mathbf{A}_{12} \\ \mathbf{A}_{12}^T & \mathbf{A}_{22} \end{bmatrix} \begin{bmatrix} \mathbf{x}_1 \\ \mathbf{x}_2 \end{bmatrix}. \quad (43)$$

Letting $\mathbf{B} = -{}^b\mathbf{W}_n^T \mathbf{M}^{-1} {}^b\mathbf{W}_n$, then \mathbf{A}_{11} , \mathbf{A}_{12} , and \mathbf{A}_{22} are defined as follows:

$$\mathbf{A}_{11} = \mathbf{M}^{-1} + \mathbf{M}^{-1} {}^b\mathbf{W}_n \mathbf{B}^{-1} {}^b\mathbf{W}_n^T \mathbf{M}^{-1} \quad (44)$$

$$\mathbf{A}_{12} = -\mathbf{B}^{-1} {}^b\mathbf{W}_n^T \mathbf{M}^{-1} \quad (45)$$

$$\mathbf{A}_{22} = \mathbf{B}^{-1}. \quad (46)$$

Substituting back into inequalities (39) yields a standard LCP(F , f) with F , f , and z given as follows:

$$F = \begin{bmatrix} {}^u\mathbf{W}_n^T \mathbf{A}_{11} {}^u\mathbf{W}_n & {}^u\mathbf{W}_n^T \mathbf{A}_{11} {}^u\mathbf{D} & {}^u\mathbf{W}_n^T \mathbf{A}_{11} {}^b\mathbf{D} & 0 & 0 \\ {}^u\mathbf{D}^T \mathbf{A}_{11} {}^u\mathbf{W}_n & {}^u\mathbf{D}^T \mathbf{A}_{11} {}^u\mathbf{D} & {}^u\mathbf{D}^T \mathbf{A}_{11} {}^b\mathbf{D} & {}^u\mathbf{E} & 0 \\ {}^b\mathbf{D}^T \mathbf{A}_{11} {}^u\mathbf{W}_n & {}^b\mathbf{D}^T \mathbf{A}_{11} {}^u\mathbf{D} & {}^b\mathbf{D}^T \mathbf{A}_{11} {}^b\mathbf{D} & 0 & {}^b\mathbf{E} \\ \mathbf{U} & -{}^u\mathbf{E}^T & 0 & 0 & 0 \\ 0 & 0 & -{}^b\mathbf{E}^T & 0 & 0 \end{bmatrix}$$

$$f = \begin{bmatrix} {}^u\mathbf{W}_n^T \mathbf{r} + {}^u\Psi_n^{(l)}/h + \frac{\partial {}^u\Psi_n^{(l)}}{\partial t} \\ {}^u\mathbf{D}^T \mathbf{r} \\ {}^b\mathbf{D}^T \mathbf{r} \\ 0 \\ {}^b\boldsymbol{\beta}_{\max} \end{bmatrix} \quad z = \begin{bmatrix} {}^u\mathbf{p}_n \\ {}^u\boldsymbol{\beta} \\ {}^b\boldsymbol{\beta} \\ {}^u\boldsymbol{\sigma} \\ {}^b\boldsymbol{\sigma} \end{bmatrix}$$

where

$$\mathbf{r} = \mathbf{A}_{11} \left(\mathbf{M} \mathbf{v}^{(l)} + \mathbf{p}_{\text{ext}} \right) + \mathbf{A}_{12} \left({}^b\Psi_n^{(l)}/h + \frac{\partial {}^b\Psi_n^{(l)}}{\partial t} \right). \quad (47)$$

Note that it is known that when there are no joints (*i.e.*, rows three and five are removed from F , f , and z and columns three and five are removed from F) and the sum ${}^u\Psi_n^{(l)}/h + \frac{\partial {}^u\Psi_n^{(l)}}{\partial t}$ is nonnegative, then a solution always exists.

4 Example Problem

Figure 7 shows an elevation view of a rough uniform sphere of unit radius and mass in contact with a fixed horizontal plane in a uniform gravitational field. Since there are no joints, ${}^b\Psi_n$ is empty, and consequently, so are ${}^b\mathbf{W}_n$, ${}^b\mathbf{D}$, ${}^b\mathbf{E}$, \mathbf{x}_2 , \mathbf{A}_{12} , \mathbf{A}_{22} , and \mathbf{B} . This example was chosen, because of the existence of easily obtainable closed-form solutions of the dynamic motion of the sphere for certain initial conditions.

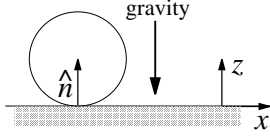


Figure 7. Sphere on a Fixed Horizontal Plane.

Let the plane coincide with the xy -plane of a (right-handed) inertial frame, with the inertial z -direction upward. Thus the normal direction \hat{n} at the contact, will always points in the inertial z -direction and will pass through the center of the sphere. Thus the gap function is independent of time and is given by the following simple expression: ${}^u\Psi_n(q) = q_3 - 1$, where q_3 is the z -coordinate of the center of the sphere. The coefficient of friction was assumed to have a constant value of 0.2. The \hat{t} and \hat{o} directions will always lie in the xy -plane, and we chose their directions to be rotated $\frac{\pi}{4}(R)$ about the z -axis from the inertial x and y axes⁷. The matrices \mathbf{M} , ${}^u\mathbf{W}_n$, ${}^u\mathbf{D}$, ${}^u\mathbf{E}$, and \mathbf{U} can be seen to be constant throughout the motion. For this problem, the various matrices are:

$$\mathbf{M} = \begin{bmatrix} \mathbf{I} & \mathbf{0} \\ \mathbf{0} & \frac{2}{5}\mathbf{I} \end{bmatrix}, \quad {}^u\mathbf{W}_n = \begin{bmatrix} 0 \\ 0 \\ 1 \\ 0 \\ 0 \\ 0 \end{bmatrix}, \quad {}^u\mathbf{D} = \begin{bmatrix} 1 & -1 & 0 & 0 \\ 0 & 0 & 1 & -1 \\ 0 & 0 & 0 & 0 \\ 0 & 0 & 1 & -1 \\ -1 & 1 & 0 & 0 \\ 0 & 0 & 0 & 0 \end{bmatrix},$$

$${}^u\mathbf{E} = \begin{bmatrix} 1 \\ 1 \\ 1 \\ 1 \end{bmatrix}, \quad \mathbf{U} = 0.2, \quad \mathbf{g}_{\text{ext}} = \begin{bmatrix} 0 \\ 0 \\ -9.81 \\ 0 \\ 0 \end{bmatrix}.$$

⁷This rotation was caused by a quirk in our Matlab code, but is only relevant in the discussion of the results plotted in Figures 8 and 9.

In order to obtain a close-form solution, the sphere was released in contact with the plane and translating in the x -direction. The corresponding time-stepping LCP(\mathbf{F} , \mathbf{f}) has with \mathbf{F} , \mathbf{f} , and \mathbf{z} given as follows:

$$\mathbf{F} = \begin{bmatrix} 1 & 0 & 0 & 0 & 0 & 0 \\ 0 & 3.5 & 3.5 & 0 & 0 & 1 \\ 0 & 3.5 & 3.5 & 0 & 0 & 1 \\ 0 & 0 & 0 & 3.5 & 3.5 & 1 \\ 0 & 0 & 0 & 3.5 & 3.5 & 1 \\ 0.2 & -1 & -1 & -1 & -1 & 0 \end{bmatrix} \quad (48)$$

$$\mathbf{f} = \begin{bmatrix} \nu_3^{(l)} + \psi_n^{(l)}/h - 9.81 h \\ \nu_1^{(l)} - \nu_5^{(l)} \\ -\nu_1^{(l)} + \nu_5^{(l)} \\ \nu_2^{(l)} + \nu_4^{(l)} \\ -\nu_2^{(l)} - \nu_4^{(l)} \\ 0 \end{bmatrix}, \quad \mathbf{z} = \begin{bmatrix} {}^u p_n^{(l+1)} \\ \beta_1^{(l+1)} \\ \beta_2^{(l+1)} \\ \beta_3^{(l+1)} \\ \beta_4^{(l+1)} \\ {}^u \sigma^{(l+1)} \end{bmatrix} \quad (49)$$

where the subscript i has been dropped, since there is only one contact, $(\nu_1, \nu_2, \nu_3) = (v_x, v_y, v_z)$ are the x -, y -, and z -components of the linear velocity of the center of the sphere, and $(\nu_4, \nu_5, \nu_6) = (\omega_x, \omega_y, \omega_z)$ and the x -, y -, and z -components of the angular velocity of the sphere.

With the following initial conditions:

$$\begin{aligned} \text{initial configuration: } \mathbf{q} &= [0 \ 0 \ 1 \ | \ 1 \ 0 \ 0 \ 0]^T \\ \text{initial velocity: } \boldsymbol{\nu} &= [2 \ 0 \ 0 \ | \ 0 \ 0 \ 0]^T \end{aligned} \quad (50)$$

the exact solution of the sphere's motion was found⁸. The sphere initially slides in the x -direction, gathering angular velocity in the y -direction until the transition time, $t_{\text{trn}} = \frac{2v_{x0}}{7\mu g} \approx 0.291$, where v_{x0} is the initial velocity in the x -direction and $g = 9.81\text{m/s}^2$ is the acceleration due to gravity. After the transition time, the sphere rolls with constant velocity in the x -direction and angular velocity $\omega_y = \frac{5}{7}v_{x0} \approx 1.429$ in the y -direction. The remaining 4 velocity components are zero.

The numerical solution was computed over the time interval $[0, 0.6]$ with $h = 0.12$. The method matched the exact velocities as shown in Figure 8, which plots the sphere's velocity components on top of the exact solution (shown as dotted lines). It should be noted that our method matched the exact solution, because one of the friction directions chosen (column 2 of ${}^u\mathbf{D}$) was

⁸Note that the last for elements of initial configuration, $(1, 0, 0, 0)$, is the unit quaternion, and it's initial value has no bearing on the results in terms of forces and velocities.

pointing exactly in the $-x$ -direction. Since every nonzero friction force for this example was acting in this direction, there was no error caused by friction cone linearization. Similarly, since Ψ_n was linear, no error was generated by the linear approximation in equation (30).

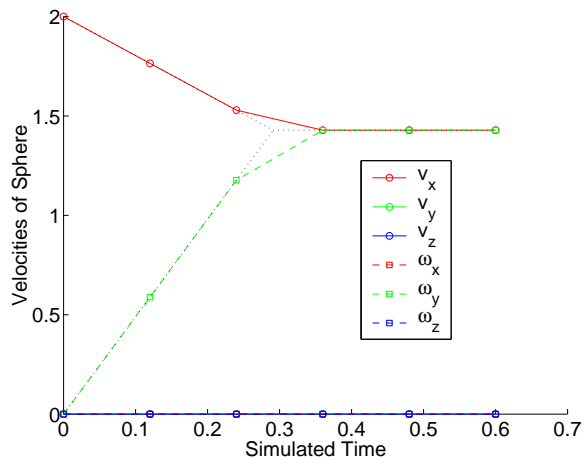


Figure 8. Analytical and Numerical Velocities with $h = 0.12$.

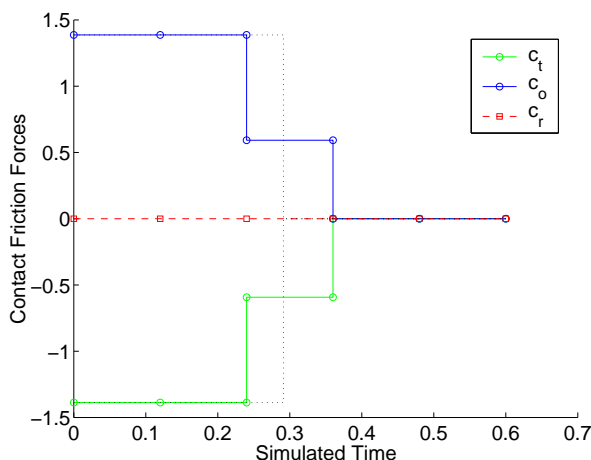


Figure 9. Analytical and Numerical Forces with $h = 0.12$.

Figure 9 shows the components of the friction force over time as predicted by our method. Note that both c_t and c_o were nonzero due to the misalignment of the \hat{t} and \hat{o} directions with respect to the x - and y -axes of the inertial frame. Again, the analytical solution is plotted with dotted lines. This example was rerun with smaller step sizes to demonstrate convergence to the exact solution.

5 Conclusion

We have presented complementarity formulations of the instantaneous and discrete-time dynamics of general, spatial, multi-rigid-body system with joints and unilateral contacts with a form of dry friction. Details on the derivation of the continuous-time or instantaneous model can be found in [8]. The extension of the instantaneous model to include a friction moment along the contact normal and discussions of other examples can be found in [9]. The formulation of the same basic discrete-time model presented here can be found in [7]. The minor extension to include load-independent dry friction in one-degree-of-freedom joints has not previously been presented. Last, a higher-order version of the discrete-time method presented here has been implemented in the software package Umbra at Sandia National Laboratories. Movies of animations produced with Umbra can be found at www.cs.rpi.edu/~trinkle.

REFERENCES

- [1] M. Anitescu and F.R. Potra. Formulating multi-rigid-body contact problems with friction as solvable linear complementarity problems. *ASME Journal of Nonlinear Dynamics*, 14:231–247, 1997.
- [2] G. Boothroyd and A.H. Redford. *Mechanized Assembly: Fundamentals of Parts Feeding, Orientation, and Mechanized Assembly*. McGraw-Hill, 1968.
- [3] R. W. Cottle, J.S. Pang, and R. E. Stone. *The Linear Complementarity Problem*. Academic Press, 1992.
- [4] S. Goyal. *Planar Sliding of a Rigid Body with Dry Friction: Limit Surfaces and Dynamics of Motion*. PhD thesis, Cornell University Department of Mechanical Engineering, January 1989.
- [5] C. Lanczos. *The Variational Principles of Mechanics*. University of Toronto Press, 1986.
- [6] J.S. Pang and J.C. Trinkle. Complementarity formulations and existence of solutions of dynamic multi-rigid-body contact problems with coulomb friction. *Mathematical Programming*, 73:199–226, 1996.
- [7] D.E. Stewart and J.C. Trinkle. An implicit time-stepping scheme for rigid body dynamics with inelastic collisions and coulomb friction. *International Journal of Numerical Methods in Engineering*, 39:2673–2691, 1996.
- [8] J.C. Trinkle, J.S. Pang, S. Sudarsky, and G. Lo. On dynamic multi-rigid-body contact problems with coulomb friction. *Zeitschrift für Angewandte Mathematik und Mechanik*, 77(4):267–279, 1997.
- [9] J.C. Trinkle, J.A. Tzitzouris, and J.S. Pang. Dynamic multi-rigid-body systems with concurrent distributed contacts: Theory and examples. *Philosophical Transactions: Mathematical, Physical, and Engineering Sciences*, 359(1789):2575–2593, December 2001.

ACKNOWLEDGMENT

This work was partially supported by NSF under grant DMS 0139701 and start-up funds provided by the School of Science, RPI. Any findings, conclusions, or recommendations expressed here are those of the author and do not necessarily reflect the views of the funding agencies. Note that portions of this paper closely follow sections in [7–9].